Aalborg Universitet

High-Rate Analysis of Symmetric L-Channel Multiple Description Coding

Zhang, Guoqiang; Østergaard, Jan; Klejsa, Janus ; Kleijn, Bastiian

High-Rate Analysis of Symmetric L-Channel Multiple Description Coding

Guoqiang Zhang, Jan Østergaard, *Member, IEEE*, Janusz Klejsa, and W. Bastiaan Kleijn, *Fellow, IEEE*

Abstract—**This paper studies the tight rate-distortion bound for L-channel symmetric multiple-description coding of a scalar Gaussian source with two levels of receivers. Each of the first-level receivers obtains κ of the L descriptions ($\kappa < L$). The second-level receiver obtains all L descriptions. We find that if the central distortion (corresponding to the second-level receiver) is much smaller than the side distortion (corresponding to the first-level receivers), the product of a function of the side distortions and the central distortion is asymptotically independent of the redundancy between the descriptions. Using this property, we analyze the asymptotic behavior of a practical multiple-description lattice vector quantizer (MDLVQ). Our analysis includes the treatment of the MDLVQ system from a new geometric viewpoint, which results in an expression for the side distortions using the normalized second moment of a sphere of higher dimensionality than the quantization space. The expression of the distortion product derived from the lower bound is then applied as a criterion to assess the performance loss of the considered MDLVQ system. In principle, the efficiency of other practical MD systems can also be evaluated using the derived distortion product.**

Index Terms—**Multiple description coding, high-rate quantization, lattice quantizer.**

I. INTRODUCTION

MULTIPLE description coding (MDC) is an effective joint source-channel coding method that addresses the loss of packets commonly observed in packet networks. Whereas early work on MDC mainly focused on the two-channel (two-description) case (e.g., [1]–[3]), the general multi-channel case has received increased attention in recent years. The general case is relevant since with increasing packet-loss rate the optimal MDC configuration contains an increasingly large number of channels [4]. The main aim of this paper is to derive a simple approximation of the rate-distortion lower bound for the multi-channel case and to apply the lower-bound approximation in the performance assessment of practical MD systems.

Let us elaborate on the context of the problem in more detail. L-channel multiple-description (MD) schemes are designed for communication systems with L channels connecting the source and the destination. Each channel is assumed to provide an independent means of transmission. A theoretical challenge within the MD problem is to understand the performance limits concerning the trade-off between transmission rate and reconstruction quality. We refer to the distortion when all L descriptions are received as the *central distortion* and to distortions when fewer descriptions are received as *side distortions*. The distortion corresponding to a single received description is referred to as *individual side distortion*. In this work, we focus on the symmetric MD scenario, which assumes that the per-channel rates are the same across the L channels and that the distortion only depends upon the number of received descriptions.

The rate-distortion lower bound for the two-channel case has been explored extensively (e.g., [1]–[3]). Ozarow [2] constructed a tight lower bound for the specialized case of a scalar Gaussian source and the squared-error distortion criterion. The tight lower bound was further investigated in [5] for a symmetric descriptions scenario. A useful high-rate result was provided that the product of the central distortion and the side distortion is asymptotically determined by the transmission rate. The advantage of this property is that it gives an asymptotically accurate approximation of the theoretical lower bound. Thus, it serves as a simple means of relating the performance of practical MD schemes to the lower bound of [2]. The asymptotic behavior of the distortion product has been utilized widely as a tool to assess the efficiency of practical two-channel MD systems. For example, Vaishampayan et al. [6] proposed an MD lattice vector quantizer (MDLVQ) that exploits the geometry of lattices. They showed that, in the high-rate regime, the distortion product of the quantizer behaves similarly to the bound and that the gap to the theoretical bound vanishes with increasing dimensionality. The present paper extends this work to the symmetric L-channel case.

Before we describe the context of our work, we briefly review the progress on deriving the rate-distortion lower bound and on designing practical MD quantizers for the L-channel case. The characterization of the (tight) rate-distortion bound for a general L-channel MDC still remains an open problem. Instead, the main focus has been on special cases, e.g., the case where only a subset of the distortion constraints is of concern [7]–[9]. In particular in [9], Wang and Viswanath addressed the symmetric descriptions scenario with two levels of receivers. Each of the first-level receivers obtains κ of the L descriptions ($\kappa < L$). For a particular κ, the number of first-level receivers is thus $\binom{L}{\kappa}$. The second-level receiver obtains all the L descriptions. For the considered MD scenario, the

G. Zhang and J. Klejsa are with the School of Electrical Engineering, KTH-Royal Institute of Technology, SE-100 44 Stockholm, Sweden (e-mail: guoqiang.zhang@ee.kth.se; janusz.klejsa@ee.kth.se).

J. Østergaard is with the Department of Electronic Systems, Aalborg University, 9220 Aalborg, Denmark (janoe@ieee.org).

W. B. Kleijn is with the School of Electrical Engineering, KTH–Royal Institute of Technology, SE-100 44 Stockholm, Sweden and also with School of Engineering and Computer Science, Victoria University of Wellington, New Zealand (e-mail: bastiaan@kth.se).

tight lower bound has been derived for a vector Gaussian source with the quadratic distortion criterion.

The design of practical L-channel MDLVQ systems was addressed in [4], [10]. The index assignment was recognized to play an important role in the system design. Besides the index-assignment-based methods, several other L-channel MD systems have been proposed in [11]–[13]. Unlike the two-channel case, no effective tool has yet been developed for evaluating the performance loss of practical L-channel MD schemes. Therefore, this paper aims at filling this gap by extending the work done in [5] for the two-channel case.

Formally, the present work provides an asymptotic analysis of the tight rate-distortion lower bound derived in [9] for symmetric scalar Gaussian MDC with two levels of receivers. A simple approximation, which is asymptotically tight, of the rate-distortion bound is derived and then utilized to assess the efficiency of a practical MDLVQ scheme [10]. The performance of the MDLVQ scheme [10] is investigated using a new geometric viewpoint on the index assignment. It should be noted that the derived lower-bound approximation is general, and that its application is not limited to the practical system of [10].

We now describe our contributions in more detail. The work of [9] provides two different expressions for a tight lower bound. We analyze one expression and find that if the central distortion is much smaller than the side distortion, the product of a function of the side distortion and the central distortion is asymptotically independent of the redundancy among the descriptions. The derived product is in fact an approximation of the tight lower-bound.

The MD scheme [10] is selected as an example application as it represents the state-of-the-art in the design of L-channel MDLVQ schemes. For the considered scheme, we present a new geometric evaluation of its performance. Suppose an n-dimensional random vector with i.i.d. components is to be encoded, and the mean squared error is considered. The geometric analysis shows that the side distortions are characterized by $G(S_{Ln-n})$, the normalized second moment of a sphere in $Ln - n$ dimensions, as compared to the fact that the central distortion is characterized by $G(\Lambda)$, the normalized second moment of a lattice Λ used for quantization. The performance loss of the scheme is evaluated by comparing the lower-bound approximation (the distortion product) and that of the scheme.

The remainder of this paper is organized as follows. Section II is devoted to the analysis of the MD lower bound. Both the algebraic duality of the two lower-bound expressions and the asymptotic behavior of the distortion product are addressed in this section. The new performance analysis for MDLVQ systems is presented in Section III. The performance loss of the system is discussed w.r.t. the new formulation of the lower bound. Conclusions are provided in section IV.

The notations used in this paper are summarized here. Lower case letters denote scalars, and boldface lower case letters denote vector random variables. Boldface upper case letters are used to denote matrices. Specifically, we use $\boldsymbol{I}$ and $\boldsymbol{0}$ to denote the identity matrices and the all-zero matrices, respectively. We also use $\boldsymbol{H}$ to denote all-one matrices. The superscript t refers to the matrix transpose operation and $|\cdot|$

refers to the determinant operation if not explicitly stated otherwise. The notation $\|\cdot\|$ represents the l_2 norm. The logarithms are to base e, unless otherwise specified.

II. ANALYSIS OF MULTIPLE DESCRIPTION LOWER BOUND

In this section, we analyze the scalar Gaussian MD lower bound on the sum-rate [9] when only two levels of receivers are concerned. In the past few years, many researchers have focused on characterizing the MD rate-distortion lower bound for Gaussian sources [7]–[9]. One reason is that Gaussian sources were shown to give the worst performance under first and second moments [3], [8]. This property indicates that knowing the performance limit for Gaussian sources aids in the understanding of the performance for other sources.

In the analysis, we only consider the symmetric descriptions scenario (i.e., the distortion constraint is only related to the number of descriptions and the per-channel rates are the same). Our main goal is to derive a simple and useful approximation of the MD lower bound which facilitates the evaluation of the efficiency of practical MD systems. In order to achieve this goal, we study the asymptotic behavior of the lower bound under a high-rate regime.

For the considered scenario, Wang and Viswanath in [9] provided two different expressions for the same tight lower bound for encoding a vector Gaussian source, namely the inner-bound expression and the outer-bound expression. We investigate the inner-bound expression by specifying the information source to be scalar Gaussian. The motivation for considering the inner-bound expression (over the outer-bound expression) is that the asymptotic analysis is more intuitive. In principle, one can alternatively study the outer-bound expression, which should produce the same result. In fact, the asymptotic analysis in our conference paper [14] was performed on the outer-bound expression for the special case of $\kappa = 1$.

In the following, we first introduce the inner-bound expression [9]. We then present the asymptotic analysis of the lower-bound. A simple approximation of the lower bound is derived.

A. Preliminaries

Suppose the information source to be encoded is a zero-mean random Gaussian variable x with variance σ_x^2. We study the symmetric MD problem with the central receiver and $\binom{L}{\kappa}$ first-level receivers each of which corresponds to a particular case that a subset of κ of the L total descriptions are received. Mathematically, this implies that only two distortion constraints will be considered, one for the central receiver and the other for the second-level receivers. Denote P as a subset of the L descriptions, i.e., $P \subseteq \{1, \ldots, L\}$. Considering the minimum mean squared error (MMSE) criterion, we denote the distortion constraints as $\bar{d}_{(L,\kappa)}, \forall P \subseteq \{1, \ldots, L\}, |P| = \kappa$ and $\bar{d}_{(L,L)}$, where $0 < \bar{d}_{(L,L)} < \bar{d}_{(L,\kappa)} < \sigma_x^2$. Let R denote the per-channel rate.

The inner-bound expression was actually derived by using a Gaussian description scheme [7]–[9]. We now briefly introduce the scheme for completeness. Let $w_1, \ldots, w_L$ be zero mean

jointly Gaussian variables independent of x, with a positive-definite covariance matrix denoted by

$$\boldsymbol{K}_w = \begin{pmatrix} \sigma^2 & -a & \dots & -a \\ -a & \sigma^2 & \ddots & \vdots \\ \vdots & \ddots & \ddots & -a \\ -a & \dots & -a & \sigma^2 \end{pmatrix}, \qquad (1)$$

where $a \geq 0$ and $\boldsymbol{K}_w$ is positive definite. The L Gaussian descriptions are then constructed as

$$u_l = x + w_l \qquad l = 1, \dots, L. \qquad (2)$$

Let $\rho = a/\sigma^2$. Using the fact that $\boldsymbol{K}_w$ is positive-definite, we deduce that $\frac{1}{L-1} > \rho \geq 0$. The parameter ρ is a normalized correlation factor between the noise variables w_l, $l = 1, \dots, L$. It controls the redundancy between the generated descriptions u_l, $l = 1, \dots, L$, which will be explained in Subsection II-B. Note that $\boldsymbol{K}_w$ is symmetric over w_l, $l = 1, \dots, L$ (i.e., the L Gaussian variables have identical variances σ^2 and identical correlations $-a$ in-between.). This is due to the fact that the symmetric descriptions scenario is being considered. To facilitate the discussion in the following, we use $\boldsymbol{K}_P$ to denote the covariance matrix of all w_l, $l \in P$, $\forall P \subseteq \{1, \dots, L\}$. Thus, $\boldsymbol{K}_P$ is of size $|P| \times |P|$. Also $\boldsymbol{K}_{\{1,\dots,L\}}$ is equivalent to $\boldsymbol{K}_w$. We present the inner-bound expression for encoding x [9] in the form of a theorem.

Theorem 2.1 (Inner-bound expression): [9, Lemma 1 and 2, Theorem 2] If there is a matrix $\boldsymbol{K}_w \succ \boldsymbol{0}$ of the form (1) such that

$$\begin{cases} \text{mmse}[x|u_l, l \in P] = \bar{d}_{(L,\kappa)} & \forall P \subset \{1, \dots, L\}, |P| = \kappa \\ \text{mmse}[x|u_1, \dots, u_L] = \bar{d}_{(L,L)} \\ \sigma_x^2 \geq a \geq 0 \end{cases}, \qquad (3)$$

then the optimal sum rate is given by

$$LR = \frac{1}{2} \log \frac{|\boldsymbol{H} \otimes \sigma_x^2 + \boldsymbol{K}_P|^{L/\kappa}}{|\boldsymbol{K}_w|}, \quad P = \{1, \dots, \kappa\}, \qquad (4)$$

where $\otimes$ denotes the Kronecker product [15].

B. Asymptotic Tight Lower Bound to the Rate-Distortion Function

From the appearance of the inner-bound expression (3)-(4), it is difficult to recognize the trade-off directly between the sum rate and the distortions. In this subsection, our goal is to provide a better understanding of the relationship of the sum-rate and the distortions by analyzing (3)-(4). In particular, a simple approximation of the lower bound is derived by assuming high-rate transmission, which will be used to evaluate a practical MD system in Section III.

We now study the inner-bound expression (3)-(4). Suppose a matrix $\boldsymbol{K}_w$ satisfies the condition (3). From estimation theory [16], it can be shown that

$$\bar{d}_{(L,\kappa)}^{-1} = \sigma_x^{-2} + (1, \dots, 1)\boldsymbol{K}_P^{-1}(1, \dots, 1)^t$$
$$\forall P \subset \{1, \dots, L\}, |P| = \kappa, \qquad (5)$$

$$\bar{d}_{(L,L)}^{-1} = \sigma_x^{-2} + (1, \dots, 1)\boldsymbol{K}_w^{-1}(1, \dots, 1)^t. \qquad (6)$$

By using Lemma A.2, (5)-(6) can be further simplified as

$$\sigma^2 - (\kappa - 1)a = \kappa(\bar{d}_{(L,\kappa)}^{-1} - \sigma_x^{-2})^{-1}, \qquad (7)$$

$$\sigma^2 - (L - 1)a = L(\bar{d}_{(L,L)}^{-1} - \sigma_x^{-2})^{-1}. \qquad (8)$$

(7)-(8) describes the relationship between $\{\sigma^2, a\}$ and the distortions $\{\bar{d}_{(L,\kappa)}, \bar{d}_{(L,L)}\}$. Correspondingly, the optimal sum rate can be rewritten as

$$LR = \frac{1}{2} \log \frac{|\boldsymbol{H} \otimes \sigma_x^2 + \boldsymbol{K}_{\{1,\dots,\kappa\}}|^{L/\kappa}}{|\boldsymbol{K}_w|} \qquad (9)$$

$$= \frac{1}{2} \log \frac{|\kappa\sigma_x^2 + \sigma^2 - (\kappa - 1)a|^{L/\kappa}}{|\sigma^2 - (L-1)a||\sigma^2 + a|^{L/\kappa-1}} \qquad (10)$$

$$= \frac{1}{2} \log \left(\frac{\kappa^N (L - \kappa)^{N(L/\kappa - 1)}}{L^{NL/\kappa} \left| \bar{d}_{(L,L)}^{-1} - \sigma_x^{-2} \right|^{-1}} \right.$$
$$\cdot \frac{\left| \sigma_x^2 + (\bar{d}_{(L,\kappa)}^{-1} - \sigma_x^{-2})^{-1} \right|^{L/\kappa}}{\left| (\bar{d}_{(L,\kappa)}^{-1} - \sigma_x^{-2})^{-1} - (\bar{d}_{(L,L)}^{-1} - \sigma_x^{-2})^{-1} \right|^{L/\kappa-1}} \left. \right) \quad (11)$$

$$= \frac{1}{2} \log \left(\frac{\kappa^N (L - \kappa)^{N(L/\kappa - 1)} |\sigma_x^2|^{L/\kappa}}{L^{NL/\kappa} |\bar{d}_{(L,L)}||\bar{d}_{(L,\kappa)} - \bar{d}_{(L,L)}|^{L/\kappa-1}} \right.$$
$$\left. \cdot \frac{|\sigma_x^2 - \bar{d}_{(L,L)}|^{L/\kappa}}{|\sigma_x^2 - \bar{d}_{(L,\kappa)}||\sigma_x^2|^{L/\kappa-1}} \right). \qquad (12)$$

In the above derivation, (10) follows from Lemma A.3, and (11) follows from (7)-(8). Finally (12) follows from Lemma A.1.

Equ. (12) completely characterizes the relationship between the optimal transmission rate R and the associated distortions $\{\bar{d}_{(L,\kappa)}, \bar{d}_{(L,L)}\}$. However, the right hand side of (12) takes a complicated form in terms of the distortions. It is highly desirable to find a good but simple approximation of (12) so that the trade-off between the transmission rate and the distortions can be easily understood.

Before presenting the asymptotic analysis to approximate (12), we first study how the central and side distortions change with ρ for a fixed transmission rate. In other words, we take the central and side distortions as functions of ρ given a transmission rate. Suppose that $\rho \in [0, 1/(L - 1))$. From Theorem 2.1, we obtain the following optimality condition on σ^2:

$$\sigma_x^2/\rho \geq \sigma^2 > 0. \qquad (13)$$

Theorem 2.1 implies that for a Gaussian test channel defined by $\rho \in [0, 1/(L - 1))$ and $\sigma^2 \in (0, \sigma_x^2/\rho]$, the optimal sum rate takes the form

$$LR = \frac{1}{2} \log \frac{[\kappa\sigma_x^2 + \sigma^2(1 - (\kappa - 1)\rho)]^{L/\kappa}}{\sigma^{2L/\kappa}[1 - (L-1)\rho](1 + \rho)^{L/\kappa-1}}. \qquad (14)$$

We now fix R in (14), and determine a support region of ρ within $[0, 1/(L - 1))$ such that (13) holds. It should be noted that for the considered case, σ^2 is a function of ρ. We consider two extreme cases, one with $\rho = 0$ and one with $\rho = \sigma_x^2/\sigma^2$. It is easily seen that when $\rho = 0$, there exists a finite σ^2

satisfying both (13) and (14). For the case that $\rho = \sigma_x^2/\sigma^2$, an expression of ρ is derived from (14), which takes the form

$$\rho = \frac{\sigma_x^2}{\sigma^2} = \frac{1 - e^{-2LR}}{L - 1 + e^{-2LR}}. \tag{15}$$

With (15), it follows that the support region of ρ for a fixed rate in (14) is $B_\rho(R) = [0, (1 - e^{-2LR})/(L - 1 + e^{-2LR})]$. Further as the rate R increases, the length of the support region increases and approaches $1/(L - 1)$. Based on (7)-(8), we consider the derivatives of $\sigma^2(1 - (\kappa - 1)\rho)$ and $\sigma^2(1 - (L - 1)\rho)$ w.r.t. ρ for $\rho \in B_\rho(R)$:

$$\frac{d}{d\rho}[\sigma^2(1 - (L-1)\rho)] = \frac{\rho\sigma^2(L - \kappa)(\sigma^2 - \sigma_x^2/\rho)}{\sigma_x^2(1 + \rho)} \le 0, \tag{16}$$

$$\begin{aligned}\frac{d}{d\rho}[\sigma^2(1 - (\kappa - 1)\rho)] &= \frac{\kappa\rho(\sigma_x^2/\rho - \sigma^2) + \sigma^2(1 + \rho)}{\sigma_x^2(1 - (L-1)\rho)(1 + \rho)} \\ &\quad \cdot (L - \kappa)\rho\sigma^2 \\ &\ge 0. \end{aligned} \tag{17}$$

By combining (7)-(8) and (16)-(17), we conclude that with increasing ρ, the corresponding central distortion decreases and the side distortion $\bar{d}_{(L,\kappa)}$ increases. In other words, the information shared between the descriptions becomes less and less as ρ increases. Particularly, for the extreme case that $\rho = \sigma_x^2/\sigma^2$, one can show from (7)-(8) and (15) that the central distortion reaches the single-description lower bound, i.e. $\bar{d}_{(L,L)} = \sigma_x^2 e^{-2LR}$. Correspondingly, the side distortion $\bar{d}_{(L,\kappa)}$ takes the form

$$\bar{d}_{(L,\kappa)} = \sigma_x^2[(L - \kappa)/L + (\kappa/L)e^{-2LR}]. \tag{18}$$

Note that when $R \to \infty$, the side distortion in (18) approaches a nonzero constant instead of 0:

$$\bar{d}_{(L,\kappa)} \to [(L - \kappa)/L]\sigma_x^2 \quad \text{as } R \to \infty. \tag{19}$$

We now consider deriving a simple approximation to (12). To achieve this goal, we study under what conditions both the central distortion $\bar{d}_{(L,L)}$ and the side distortion $\bar{d}_{(L,\kappa)}$ approach 0 with increasing transmission rate. We first fix ρ within $[0, 1/(L - 1))$. From (15), it is seen that as long as $R \ge R_0(\rho) = (1/2L)\log[(1 + \rho)/(1 - (L-1)\rho)]$, there exists σ^2 such that (13)-(14) hold. Considering (14), it is immediate that as the rate increases, σ^2 will decrease. Based on (7), it can be concluded that the side distortion $\bar{d}_{(L,\kappa)}$ approaches 0 with increasing rate when the correlation factor ρ is fixed. It follows that the central distortion also approaches 0. The above analysis implies that the quantity in (12) satisfies

$$\frac{|\sigma_x^2 - \bar{d}_{(L,L)}|^{L/\kappa}}{|\sigma_x^2 - \bar{d}_{(L,\kappa)}||\sigma_x^2|^{L/\kappa-1}} \to 1 \quad \text{as } R \to \infty. \tag{20}$$

Consequently, the rate-distortion equation (12) can be approximated as

$$\begin{aligned}&\bar{d}_{(L,L)}\bar{d}_{(L,\kappa)}^{L/\kappa-1}[1 - \bar{d}_{(L,L)}/\bar{d}_{(L,\kappa)}]^{L/\kappa-1} \\ &\approx \frac{\kappa(L - \kappa)^{L/\kappa-1}}{L^{L/\kappa}}\sigma_x^{2L/\kappa}e^{-2LR}. \end{aligned} \tag{21}$$

One observes that the rate-bound $R_0(\rho)$ is unbounded from above as ρ approaches $1/(L - 1)$. This property indicates that the convergence speed of (21) is nonuniform for different ρ. As ρ increases, higher rate is needed in (21) to obtain a good approximation. (21) serves as an asymptotic tight lower-bound approximating the lower-bound expression (3)-(4).

Note that the ratio $\bar{d}_{(L,L)}/\bar{d}_{(L,\kappa)}$ is involved in (21). We study the asymptotic behavior of the ratio for a fixed ρ. The purpose is to further simplify the approximation (21). From (7) and (8), the relation between $\bar{d}_{(L,\kappa)}$ and $\bar{d}_{(L,L)}$ is characterized as

$$\frac{\kappa[1 - (L-1)\rho]}{L[1 - (\kappa-1)\rho]} = \frac{\bar{d}_{(L,L)}(\sigma_x^2 - \bar{d}_{(L,\kappa)})}{\bar{d}_{(L,\kappa)}(\sigma_x^2 - \bar{d}_{(L,L)})}. \tag{22}$$

By using the fact that $\bar{d}_{(L,\kappa)}$ and $\bar{d}_{(L,L)}$ tend to 0 with increasing rate for a fixed ρ, (22) is approximated as

$$\bar{d}_{(L,L)}/\bar{d}_{(L,\kappa)} \to \kappa[1 - (L-1)\rho]/[L(1 - (\kappa-1)\rho)] \tag{23}$$

when $R \to \infty$. The approximation indicates that when $\rho \to 1/(L - 1)$, the ratio $\bar{d}_{(L,L)}/\bar{d}_{(L,\kappa)}$ tends to 0. In this situation, (21) can be further simplified as

$$\bar{d}_{(L,L)}\bar{d}_{(L,\kappa)}^{L/\kappa-1} \approx \kappa(L - \kappa)^{L/\kappa-1}L^{-L/\kappa}\sigma_x^{2L/\kappa}e^{-2LR}. \tag{24}$$

The approximation of the distortion product made by (24) is less accurate than (21). Let us now consider the gap between the two expressions for the extreme case when minimization of the side distortion $\bar{d}_{(L,\kappa)}$ is of primary concern. This occurs when $\rho = 0$. It is immediate from (23) that when $\rho = 0$, the distortion ratio satisfies $\bar{d}_{(L,L)}/\bar{d}_{(L,\kappa)} \to (\kappa/L)$ asymptotically in R. In this situation, the difference between (21) and (24) is characterized by a multiplier factor $(\frac{L-\kappa}{L})^{L/\kappa-1}$. Thus, as κ increases from 1 to $L - 1$, the approximation (24) of the distortion product is increasingly accurate.

Fig. 1 shows the trade-off between the central and side distortion for the case of $\kappa = 1$ and $L = 3$ for different rates. For each rate, both the exact curve and the approximated curve from (24) are plotted. It is seen that as the rate increases, the approximation accuracy is increasing. The gap between the two curves for the same rate appears only when either the reduction of the central distortion or the side distortion $\bar{d}_{(3,1)}$ is of primary concern.
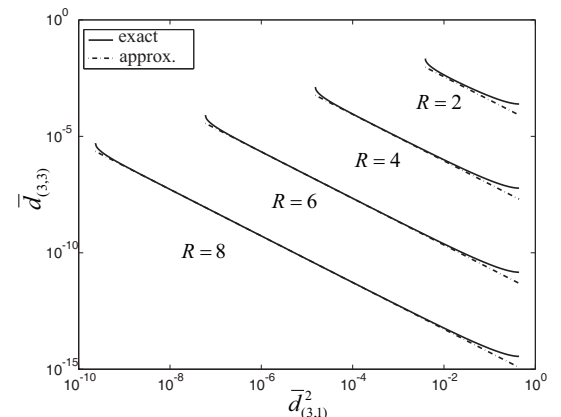

Fig. 1. Graphic depiction of the relationship of $\bar{d}_{(3,3)}$ and $\bar{d}_{(3,1)}$ for different rates. σ_x^2 is set to be 1. The per-channel rate R is measured in bits.

The characterization of MD lower bound for two-channel case was well studied in the past [3], [5], [17]. In [17], a distortion product was shown to be achievable by using the random coding argument

$$\bar{d}_{(2,2)}\bar{d}_{(2,1)}\left(1 - \bar{d}_{(2,2)}/\bar{d}_{(2,1)}\right) \approx \frac{\sigma_x^4}{4}e^{-4R}. \qquad (25)$$

For the case that $\bar{d}_{(2,2)} \ll \bar{d}_{(2,1)}$, it was shown in [5] that

$$\bar{d}_{(2,2)}\bar{d}_{(2,1)} \approx \frac{\sigma_x^4}{4}e^{-4R}, \qquad (26)$$

by analyzing the tight lower bound derived in [2]. The approximation in (26) plays an important role in practice. It is a widely used tool to measure the efficiency of MD schemes [5], [6].

Our work forms a generalization of the relations (25) and (26) by considering the multi-channel MD lower bound with two levels of receivers. Similarly to that of (26), due to the simplicity of (24), the characterization of the distortion product can serve as a useful tool for assessing symmetric L-channel MD systems. In the next section, a practical MDC system will be evaluated based on (24).

III. EVALUATION OF MDLVQ SYSTEMS

Recently, practical L-channel MDLVQ systems have been proposed, see e.g., [4], [10]. However, due to the complexity of the MD lower bound [8], [9], it is inconvenient to compare the bound directly with the performance of the developed MD systems. In this section, we consider a particular MDLVQ scheme [10] as an example to illustrate that the obtained simple approximation (24) of the lower bound can be used in the assessment of the scheme performance. It should be noted that the application of the lower-bound approximation (24) is not limited to the considered MD scheme.

For the MD system in [10], we provide a new analysis of its performance from a geometric point of view. Let n denote the dimensionality of the quantization space. We will show that the side distortions are characterized by $G(S_{Ln-n})$ (the normalized second moment of a sphere in $Ln-n$ dimensions) as compared to the quantity $G(S_n)$ for the two-channel case derived in [6]. We focus on the asymptotic behavior of the system and assess the performance loss by comparing the distortion product to (24).

It should be noted that in [10], an asymptotic analysis of the system performance is also provided. However, the expression for the side distortions in [10] takes a complicated form, and does not have a geometric interpretation. Surprisingly, we find by using algebra that our new expression for the side distortions is equivalent to that obtained in [10].

Let us first describe the basic quantization architecture for general MDLVQ systems. We then present the index assignment scheme, which is the essential part of the work in [10]. Finally we present a geometric-based analysis of the system performance.

A. System Settings

Suppose the information source $\{x[m]\}$ is an i.i.d. scalar random process with probability density function (pdf) f.

We segment the data into n-dimensional vectors $\boldsymbol{x} = (x[1], x[2], \ldots, x[n])^t$ having pdf $f_{\boldsymbol{x}}$, where

$$f_{\boldsymbol{x}} = \Pi_{i=1}^n f(x[i]).$$

We are to encode $\boldsymbol{x}$ into L descriptions, which are separately entropy-coded and transmitted to the receiving side. An MD quantizer generally involves two steps, namely, a central quantization step and an index assignment step. In the first step, the source vector $\boldsymbol{x}$ is quantized by a central quantizer $\mathcal{A}_c \subset \mathbb{R}^n$ and we denote the quantization operation by $\boldsymbol{\lambda}_c = \mathcal{Q}(\boldsymbol{x})$. Information about the central point $\boldsymbol{\lambda}_c$ is then embedded within L descriptions by use of an index assignment scheme. More formally, an injective function α maps points from the central quantizer $\mathcal{A}_c$ to a set of points in the L side codebooks. Specifically,

$$(\boldsymbol{\lambda}_0, \ldots, \boldsymbol{\lambda}_{L-1}) = \alpha(\boldsymbol{\lambda}_c), \qquad (27)$$

where $\boldsymbol{\lambda}_i \in \mathcal{A}_i$, $i = 0, \ldots, L-1$, and $\mathcal{A}_i$ is the ith side codebook. Thus, the mapping function α essentially associates every central point to an L-tuple (i.e., a set of codewords; one from each side codebook). Let $\boldsymbol{\lambda}|_0^{L-1}$ represent an L-tuple $(\boldsymbol{\lambda}_0, \ldots, \boldsymbol{\lambda}_{L-1})$. For simplicity, we denote each component of α as α_i, $i = 0, \ldots, L-1$, i.e. $\boldsymbol{\lambda}_i = \alpha_i(\boldsymbol{\lambda}_c)$. The distortions are measured using the mean squared-error criterion. Under the mapping function α, the union of central quantizer cells related to one side codeword is not necessarily convex, which is different from a conventional single-description quantizer. Informally speaking, the design objective of a good MD quantizer is to make the union of central cells corresponding to a side codeword as compact as possible so as to minimize the side distortions.

The key idea of an MDLVQ design is to impose geometrical structures onto the central quantizer and the L side codebooks. The design of the mapping function α can then be significantly simplified. Lattices are very structured. Moreover, the use of lattices for quantization can also be motivated from high-rate quantization theory. The pdf of the source under a high transmission rate is approximately constant over any particular quantization cell. Gersho [18] conjectured that the optimal entropy constrained high-rate vector quantizer for a uniform distribution over a convex bounded set has a partition whose quantization cells are congruent with some tessellating convex polytope. This establishes the basis for using lattices in vector quantization systems. In the following, we will use the term lattice codebook, when referring to a quantizer codebook defined either by a lattice or a translated lattice.

Let $\mathcal{A}_c$ be a lattice Λ_c with a fundamental region of volume $\nu = \det(\Lambda_c)$. The L side codebooks are defined to be a clean sublattice Λ_s of Λ_c with index K (i.e., the index K refers to the structure that each clean sublattice cell contains K central lattice points. see [19]), i.e. $\mathcal{A}_i = \Lambda_s$, $i = 0, \ldots, L-1$. Thus, all side codebooks are identical. The Voronoi cell of a lattice point $\boldsymbol{\lambda} \in \Lambda$ is defined as

$$V(\boldsymbol{\lambda}) = \left\{\boldsymbol{x} : \| \boldsymbol{x} - \boldsymbol{\lambda} \|^2 \leq \| \boldsymbol{x} - \boldsymbol{\lambda}' \|^2, \boldsymbol{\lambda}' \in \Lambda\right\}, \qquad (28)$$

where ties are broken in a predefined manner. We use subscripts to distinguish Voronoi cells of different lattices, e.g.,

$V_c(\boldsymbol{\lambda}_c)$ refers to the Voronoi cell of the central lattice point $\boldsymbol{\lambda}_c$. The definition of Λ_s implies that there are K central lattice points within each Voronoi cell $V_s(\boldsymbol{\lambda}_s)$ of Λ_s. Due to the regularity of Λ_c and Λ_s, one can first label the K central points within the fundamental cell $V_s(0)$. The other central points can then be labelled simply by translating the already labelled L-tuples in $V_s(0)$, i.e.

$$\alpha(\boldsymbol{\lambda}_s + \boldsymbol{\lambda}_c) = \alpha(\boldsymbol{\lambda}_c) + \boldsymbol{\lambda}_s, \quad \boldsymbol{\lambda}_s \in \Lambda_s, \boldsymbol{\lambda}_c \in V_s(0). \quad (29)$$

The index K is a trade-off factor to control the redundancy between the L descriptions. One difficulty of using (29) is to carefully select the K L-tuples for the central points in $V_s(0)$ to avoid the reuse of L-tuples. See [6] and [10] for successful applications of (29) for the two-channel and L-channel cases, respectively.

At the receiver side, if all the L descriptions are received, the inverse labeling function α^{-1} uniquely determines the central point. Due to description erasures, it may happen that the decoder receives only a subset of the L descriptions. Suppose κ of L descriptions are received. Let $\mathcal{L}^{(L,\kappa)}$ denote the set consisting of all the possible configurations. Each element $l \in \mathcal{L}^{(L,\kappa)}$ specifies a particular combination of the received descriptions, denoted by $\{\boldsymbol{\lambda}_{l_j}, j = 1, 2, \ldots, \kappa\}$. There are $|\mathcal{L}^{(L,\kappa)}| = \binom{L}{\kappa}$ such combinations. In principle, there should be $\binom{L}{\kappa}$ decoding subsystems for a particular κ. To address the decoding complexity, a simple decoding rule was proposed in [4]. When $0 < \kappa < L$, the source $\boldsymbol{x}$ is reconstructed by averaging the received descriptions, i.e.

$$\hat{\boldsymbol{x}} = \frac{1}{\kappa} \sum_{j=1}^{\kappa} \boldsymbol{\lambda}_{l_j}. \quad (30)$$

Note that this decoding process is inconsistent. If all L descriptions are received, then the inverse mapping α^{-1} is used instead of averaging. By allowing this decoding inconsistency, the design complexity of the index assignment can be significantly reduced [4]. We use $d_{(L,\kappa)}$ to denote the (mean) distortion when κ out of L descriptions are received.

The MD schemes based on (30) essentially take the minimization of the central distortion and the individual side distortions (i.e., any one out of L descriptions being received) as primary concern. The averaging operation (30) reduces the reconstruction accuracy for $1 < \kappa < L$ but not for $\kappa = 1$. Thus, the derived lower-bound approximation (24) for the case that $\kappa = 1$ is a proper figure of merit for evaluating these MD schemes.

Generally speaking, once the side codebooks are fixed, the transmission rate per channel is determined [6]. On the other hand, fixing the central quantizer specifies the central distortion $d_{(L,L)}$. The side distortions $d_{(L,\kappa)}$, $0 < \kappa < L$, are closely related to the labeling function α. How to specify α, or equivalently, propose a good index assignment that minimizes the side distortions, is the main work of designing practical MDLVQ systems.

B. Index Assignment of a MDLVQ

In this subsection, we briefly describe the index assignment scheme of the MDLVQ in [10]. The simplicity of the method

enables us to trace the geometrical properties of the index assignment.

We first introduce a so-called *scaled sublattice* $\Lambda_{s/L}$ [10], which is defined as

$$\Lambda_{s/L} = \{\boldsymbol{\lambda}_{s/L}|\ \boldsymbol{\lambda}_{s/L} = \boldsymbol{\lambda}_s/L, \boldsymbol{\lambda}_s \in \Lambda_s\}. \quad (31)$$

It is immediate that $\Lambda_s \subset \Lambda_{s/L}$. Denote Λ_s^L as the L-ary Cartesian product of Λ_s, i.e., $\Lambda_s^L = \Lambda_s \times \Lambda_s \times \cdots \times \Lambda_s$. It can be shown that the centroid (average value) of any L-tuple $\boldsymbol{\lambda}|_0^{L-1}$ from Λ_s^L is a scaled sublattice point. An onto mapping function β from Λ_s^L to $\Lambda_{s/L}$ can then defined as

$$\beta(\boldsymbol{\lambda}|_0^{L-1}) = \frac{1}{L} \sum_{i=0}^{L-1} \boldsymbol{\lambda}_i. \quad (32)$$

Each lattice point of $\Lambda_{s/L}$ is associated with many L-tuples. The scaled sublattice $\Lambda_{s/L}$ can be interpreted as a centroid distribution of the L-tuples over the space $\mathbb{R}^n$. Thus, by exploiting (32), the β function provides a unified way to arrange the L-tuples used for index assignment. Note that the L-tuples have different "spread", i.e. some are more compact than others. A distance criterion is defined to measure the spread of an L-tuple [10], that is f

$$J(\boldsymbol{\lambda}|_0^{L-1}) = \sum_{i=0}^{L-1} \| \beta(\boldsymbol{\lambda}|_0^{L-1}) - \boldsymbol{\lambda}_i \|^2 . \quad (33)$$

We refer to this criterion as a *spread measurement*. By exploiting (33), the L-tuple candidates that have the same centroid can then be ordered. Informally, L-tuples with smaller spread are favored in the index assignment.
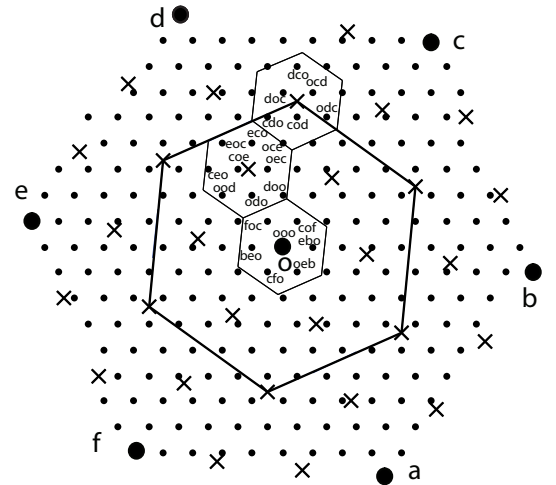
Fig. 2. Three-description index assignment for the lattice A_2 with index $K = 73$. Points of Λ_c, Λ_s and $\Lambda_{s/3}$ are denoted by $\cdot$, $\bullet$ and $\times$, respectively. The Voronoi cell $V_s(0)$ is indicated by the big hexagon in the figure.

The index assignment of the K central points in $V_s(0)$ proceeds in two steps. First, the central points are quantized to the nearest points of $\Lambda_{s/L}$. It was shown in [10] that if Λ_s is a clean sublattice of Λ_c, no central-lattice points lie on the cell boundary of $\Lambda_{s/L}$. This establishes that each central point is associated with a scaled sublattice point $\Lambda_{s/L}$ without

ambiguity. As $\Lambda_{s/L}$ is obtained by scaling Λ_s by a factor L, the fundamental Voronoi cell $V_s(0)$ contains L^n different scaled sublattice points up to translations $\{\boldsymbol{\lambda}_s - \boldsymbol{\lambda}'_s : \boldsymbol{\lambda}_s, \boldsymbol{\lambda}'_s \in \Lambda_s\}$.

Second, we label the central points within each scaled sublattice Voronoi cell $V_{s/L}(\boldsymbol{\lambda}_{s/L})$, $\boldsymbol{\lambda}_{s/L} \in V_s(0)$. The central points are assigned to the L-tuples that have the centroid $\boldsymbol{\lambda}_{s/L}$ and have a small spread as defined in (33). With this, when a subset of the descriptions is lost, the averaging operation in (30) results in a reconstruction point close to the corresponding central point. Fig. 2 displays the index assignment for the three-channel case for an A_2 lattice. By applying (29), all central points can be labeled systematically. This approach guarantees that no L-tuple is reused, thus assuring that the function α is a one-to-one mapping.

C. The Geometry of L-tuples

In this section, we revisit the index assignment and expose the geometry of the L-tuples to facilitate the performance analysis of the MD scheme. Note that each L-tuple is of dimension Ln (in integer space). The requirement to avoid the reusage of L-tuples in (29) essentially imposes an additional constraint on the L-tuple candidates, which will be shown to reduce the dimensionality of the valid candidates to $Ln - n$. For the index assignment considered, the constraint is realized by the restriction of the centroids of the L-tuples. Furthermore, the sublattice Λ_s has its lattice points uniformly distributed over space. This regularity implicitly imposes a structure to the valid L-tuple (of dimension $Ln - n$) candidates. We find that the new structure can be described by a lattice in $Ln - n$ dimensional space. Each valid L-tuple is a point of this new lattice. The reason to study the new lattice is to better understand the index assignment.

We now consider deriving the new lattice structure. We study the spread measurement for a particular L-tuple. Suppose the generator matrix of the sublattice Λ_s is $\gamma\boldsymbol{G}$, where $\boldsymbol{G}$ satisfies the condition that the matrix $\boldsymbol{M} = \boldsymbol{G}\boldsymbol{G}^t$ is an integer matrix. The parameter γ determines the Voronoi cell size of Λ_s. A lattice generated with such matrix $\boldsymbol{G}$ is called an *integral lattice* [19, page 47]. The volume of a Voronoi cell $V_s(\boldsymbol{\lambda}_s)$ is related to $\boldsymbol{M}$ by [19, page 4]

$$K\nu = \sqrt{\gamma^{2n}|\boldsymbol{M}|}. \tag{34}$$

Let us denote the L side lattice codebooks by

$$\Lambda_i = \left\{ \boldsymbol{z}_i^t \gamma\boldsymbol{G} | \quad \forall \boldsymbol{z}_i \in \mathbb{Z}^n \right\}, \ i = 0, 1, \ldots, L-1, \tag{35}$$

where $\boldsymbol{z}_i$ specifies the coordinates in the i-th codebook. From (31), the scaled sublattice takes the form of

$$\Lambda_{s/L} = \left\{ \frac{1}{L}\boldsymbol{y}^t \gamma\boldsymbol{G} | \quad \forall \boldsymbol{y} \in \mathbb{Z}^n \right\}. \tag{36}$$

Using (35) and (36), the spread measurement of an L-tuple $\boldsymbol{\lambda}|_0^{L-1}$ in (33) can then be reformulated as

$$J(\boldsymbol{\lambda}|_0^{L-1}) = \sum_{i=0}^{L-1} \| \boldsymbol{z}_i^t \gamma\boldsymbol{G} - \frac{1}{L}\boldsymbol{y}^t \gamma\boldsymbol{G} \|^2, \tag{37}$$

$$\text{subject to } \frac{1}{L}\boldsymbol{y}^t \gamma\boldsymbol{G} = \frac{1}{L}\sum_{i=0}^{L-1} \boldsymbol{z}_i^t \gamma\boldsymbol{G}.$$

After some algebra, it can be shown that (37) can be further simplified to

$$J(\boldsymbol{\lambda}|_0^{L-1}) = \gamma^2 (\check{\boldsymbol{z}} - \check{\boldsymbol{y}})^t \check{\boldsymbol{M}} (\check{\boldsymbol{z}} - \check{\boldsymbol{y}}), \tag{38}$$

where

$$\check{\boldsymbol{M}} = \begin{bmatrix} 2 & 1 & 1 & \ldots & 1 \\ 1 & 2 & 1 & \ldots & 1 \\ 1 & 1 & 2 & \ddots & \vdots \\ \vdots & \vdots & \ddots & \ddots & 1 \\ 1 & 1 & \ldots & 1 & 2 \end{bmatrix} \otimes \boldsymbol{M}, \tag{39}$$

$$\check{\boldsymbol{z}} = [\ \boldsymbol{z}_0^t \quad \boldsymbol{z}_1^t \quad \ldots \quad \boldsymbol{z}_{L-2}^t\ ]^t, \tag{40}$$

$$\check{\boldsymbol{y}} = \frac{1}{L}[\ \boldsymbol{y}^t \quad \boldsymbol{y}^t \quad \ldots \quad \boldsymbol{y}^t\ ]^t. \tag{41}$$

The matrix before $\otimes$ is of size $(L-1) \times (L-1)$, which is the Gram matrix of an A_{L-1} lattice [19]. As the Gram matrix of a lattice is always positive definite, $\check{\boldsymbol{M}}$ is thus a positive definite matrix with dimensionality $(L-1)n$. This implies that there always exists a matrix $\check{\boldsymbol{G}}$ such that $\check{\boldsymbol{M}} = \check{\boldsymbol{G}}\check{\boldsymbol{G}}^t$. Regardless of the scalar γ^2, the expression for $J(\boldsymbol{\lambda}_0^{L-1})$ in (38) can be associated with a new integral lattice Λ_{tuple} with a translation $\boldsymbol{s} = \check{\boldsymbol{G}}^t \check{\boldsymbol{y}}$. The generator matrix of Λ_{tuple} is $\check{\boldsymbol{G}}$ (note that an integral lattice only requires that its Gram matrix has integer entries, not its generator matrix [19, page 47]). We refer to the new lattice as a *tuple lattice* since each lattice point is associated with an L-tuple candidate. The introduction of the tuple lattice helps to visualize the distribution of the valid L-tuple candidates. Intuitively, the L-tuple candidates are distributed as lattice points within $Ln - n$ dimensional balls. It should be noted that the recognition of the new lattice is due to the regularity of the index assignment in (29) and the side lattice codebooks. The expression in (38) can be interpreted as the squared l_2 norm of a point of $\Lambda_{tuple} - \boldsymbol{s}$ up to a multiplying factor. The search for good L-tuples is essentially reduced to selecting the points of $\Lambda_{tuple} - \boldsymbol{s}$ with small squared l_2 norms.

Since we relate L-tuples to lattice points of Λ_{tuple}, we need to study the density of the lattice points in $Ln - n$ dimensional balls. This is closely related to the side distortions. It is desirable to design a tuple lattice such that its lattice points are as compact as possible. The characterization of the compactness of an integral lattice was given by [6], which we present in the following proposition.

Proposition 3.1: Let ν' be the volume of a Voronoi cell of an integral lattice Λ in $\mathbb{R}^n$. Denote $\mathcal{V}_n$ as the volume of a sphere of unit radius in $\mathbb{R}^n$. The number $S(m)$ of lattice points in the first m shells (the mth shell refers to a spherical shell with the square of the radius being m.) of the lattice Λ is approximately $S(m) = \frac{\mathcal{V}_n m^{\frac{n}{2}}}{\nu'}(1 + o(1))$, where $\lim_{m \to \infty} o(1) = 0$.

Proposition 3.1 provides a simple approximation for the number of points within the first m shells of a lattice. It further indicates that the density of the lattice points is fully characterized by the volume ν' of a Voronoi cell. A small ν' corresponds to a desirable high density of the lattice points.

In our work, the lattice in question is Λ_{tuple}, of which the volume of a Voronoi cell is given by

$$\sqrt{|\check{\boldsymbol{M}}|} = \sqrt{L^n |\boldsymbol{M}|^{L-1}}. \tag{42}$$

It can be seen that both L and the lattice structure (captured by $\boldsymbol{M}$) affects the compactness of the lattice points.

Note that the centroid of the L-tuple $\boldsymbol{\lambda}|_0^{L-1}$ (corresponding to a scaled sublattice point) determines the translation vector $\boldsymbol{s}$. By observing (38) and (41), one can see that when a component of the coordinate vector $\boldsymbol{y}$ is modified by adding a multiple of L, the translated lattice geometry $\Lambda_{tuple} - \boldsymbol{s}$ remains the same. This is because the relative arrangement of the scaled sublattice points and Λ_s exhibits periodicity over space. In total, there are L^n different translated lattice geometries, one for each lattice point $\boldsymbol{\lambda}_{s/L}$ within $V_s(0)$.

D. Asymptotic Analytic Performance

Based on the newly discovered tuple lattice, we present an asymptotic analysis of the index-assignment scheme proposed in [10]. In particular, we show that the side distortions are characterized by the normalized second moment $G(S_{Ln-n})$ of a sphere of dimensionality $Ln - n$. Finally we show that our expression for the side distortions is equivalent to that of [10].

We begin by considering the transmission rate. Let R_c be the central rate required to address the central quantizer $\mathcal{A}_c$. Let $\mathcal{H}(\cdot)$ denote the entropy of a discrete random variable. By exploiting high-rate quantization theory, $R_c = \mathcal{H}(\mathcal{Q}(\boldsymbol{x}))/n$ can be approximated as

$$R_c \approx h(f) - (1/n)\log(\nu), \tag{43}$$

where $h(f)$ is the differential entropy of the source. The transmission rate R per description of the MD system can be evaluated by considering the quantity $\mathcal{H}(\alpha_i(Q(\boldsymbol{x})))/n$. Strictly speaking, the rate R is regulated by the index-assignment. However, again by assuming high-rate quantization, it can be shown [6] that R has a simple expression, given as

$$R \approx h(f) - (1/n)\log(K\nu). \tag{44}$$

Note that the term $K\nu$ is simply the volume of the fundamental region $V_s(0)$ of the sublattice Λ_s. Thus, R is essentially determined by the side lattice codebook. From (43) and (44), it is seen that the relation between R_c and R is

$$R \approx R_c - (1/n)\log(K). \tag{45}$$

Since the total rate in the MD system is $LR = LR_c - (L/n)\log(K)$, the rate overhead is given by $(L-1)R_c - (L/n)\log(K)$. It is seen that the index K indeed controls the redundancy.

Next we study the central distortion $d_{(L,L)}$ and side distortions $d_{(L,\kappa)}, 0 < \kappa < L$. The central distortion (per dimension) is determined by the central codebook Λ_c, which satisfies

$$d_{(L,L)} \approx G(\Lambda_c)\nu^{2/n}, \tag{46}$$

where $G(\Lambda_c)$ represents the normalized second moment of the central lattice. The regularity of the labelling function α leads to relatively simple expressions of the side distortions. We will use $d_{(L,\kappa)}^{(l)}$ to denote the distortion for a particular configuration l from the set of configurations where κ out of L descriptions are received, i.e. $l \in \mathcal{L}^{(L,\kappa)}$. By applying (30), $d_{(L,\kappa)}^{(l)}$ can be expressed as

$$d_{(L,\kappa)}^{(l)} = \frac{1}{n} \sum_{\boldsymbol{\lambda}_c \in \Lambda_c} \int_{V_c(\boldsymbol{\lambda}_c)} f_{\boldsymbol{x}}(\boldsymbol{x}) \parallel \boldsymbol{x} - \frac{1}{\kappa} \sum_{i=1}^{\kappa} \boldsymbol{\lambda}_{l_i} \parallel^2 d\boldsymbol{x}. \tag{47}$$

Thus, the (mean) side distortion $d_{(L,\kappa)}$ can be expressed in terms of $d_{(L,\kappa)}^{(l)}$ as

$$d_{(L,\kappa)} = \frac{1}{\binom{L}{\kappa}} \sum_{l \in \mathcal{L}^{(L,\kappa)}} d_{(L,\kappa)}^{(l)}. \tag{48}$$

Under the high rate assumption, one can show that the side distortion can be approximated as [4]

$$d_{(L,\kappa)} \approx d_{(L,L)}$$
$$+ \frac{1}{\binom{L}{\kappa}} \frac{1}{Kn} \sum_{\boldsymbol{\lambda}_c \in V_s(0)} \sum_{l \in \mathcal{L}^{(L,\kappa)}} \left[\parallel \boldsymbol{\lambda}_c - \frac{1}{\kappa} \sum_{i=1}^{\kappa} \boldsymbol{\lambda}_{l_i} \parallel^2 \right] \tag{49}$$

The second term in (49) can be simplified further as shown in [10], which leads to a new expression for the side distortion, i.e.,

$$d_{(L,\kappa)} \approx d_{(L,L)} + d_1 + \frac{L-\kappa}{L\kappa(L-1)} d_2 \tag{50}$$

where

$$d_1 = \frac{1}{Kn} \sum_{\boldsymbol{\lambda}_c \in V_s(0)} \parallel \boldsymbol{\lambda}_c - \bar{\boldsymbol{\lambda}}(\boldsymbol{\lambda}_c) \parallel^2, \tag{51}$$

$$d_2 = \frac{1}{Kn} \sum_{\boldsymbol{\lambda}_c \in V_s(0)} \sum_{i=0}^{L-1} \parallel \boldsymbol{\lambda}_i(\boldsymbol{\lambda}_c) - \bar{\boldsymbol{\lambda}}(\boldsymbol{\lambda}_c) \parallel^2, \tag{52}$$

where the L-tuple assigned to $\boldsymbol{\lambda}_c$ is $\{\boldsymbol{\lambda}_i(\boldsymbol{\lambda}_c)\}_{i=0}^{L-1}$ and $\bar{\boldsymbol{\lambda}}(\boldsymbol{\lambda}_c) = \frac{1}{L} \sum_{j=0}^{L-1} \boldsymbol{\lambda}_j(\boldsymbol{\lambda}_c)$. Note that the side distortion is not dependent on the source pdf. It is fully determined by the lattice structure and the index assignment.

We consider approximating d_1 and d_2, respectively. From (33) it follows that d_2 is essentially the summation of the spread measurements. As the L-tuples are searched and arranged w.r.t. their centroids described by $\Lambda_{s/L}$, d_2 can be further decomposed with regard to the scaled sublattice points. Note that the points of Λ_c and $\Lambda_{s/L}$ are uniformly distributed over the space. We assume that each Voronoi cell $V_{s/L}(\boldsymbol{\lambda}_{s/L})$ contains approximately K/L^n central lattice points. The assumption holds when the index value K is large. We will use the term $\boldsymbol{\lambda}|_0^{L-1}(i)$, $i = 0, 1, \ldots, K/L^n - 1$ when referring to the K/L^n L-tuples used to label the central points within a Voronoi cell $V_{s/L}(\boldsymbol{\lambda}_{s/L})$ and we note that $\beta(\boldsymbol{\lambda}|_0^{L-1}(i)) = \boldsymbol{\lambda}_{s/L}$. The sum of the spread measurements of these K/L^n L-tuples can be parameterized by studying Λ_{tuple}. When K is sufficiently large, the K/L^n selected points of $\Lambda_{tuple} - \boldsymbol{s}$ can be approximated by the K/L^n selected points of Λ_{tuple}

when computing the sum of the spread measurements. The analysis can be simplified by only considering the situation that $\beta(\boldsymbol{\lambda}|_0^{K-1}(i)) = 0$, $i = 0, 1, \ldots, K/L^n - 1$. Denote the theta series [19] of Λ_{tuple} by $\Theta_{\Lambda_{tuple}}(z) = \sum_{j=0}^{\infty} B_j q^j$, where $q = e^{iz}$. The coefficient B_j indicates the number of points in the j-th shell of the lattice. Thus, we can write

$$\sum_{i=0}^{K/L^n-1} J(\boldsymbol{\lambda}|_0^{L-1}(i)) \approx \gamma^2 \sum_{j=0}^{E} j B_j, \qquad (53)$$

where we assume that $K/L^n \approx \sum_{j=0}^{E} B_j$. The parameter E indicates the maximum shell index. The main difficulty in deriving the expression for d_2 is within parameterizing the theta series of Λ_{tuple}.

Let the lattice in Proposition 3.1 be Λ_{tuple}. Then the index K is related to the shell index E in (53) by

$$K/L^n \approx \mathcal{V}_{n(L-1)} E^{\frac{n(L-1)}{2}} / \sqrt{|\check{M}|}, \qquad (54)$$

where $\mathcal{V}_{n(L-1)}$ represents the volume of a sphere with unit radius in $n(L-1)$ dimensional space as stated in Proposition 3.1. The term $\sum_{j=0}^{E} j B_j$ can also be approximated using a simple expression [6]. Specifically, using the relation $S(m) = \sum_{j=0}^{m} B_j$ and Abel's summation formula, it can be shown that

$$\sum_{j=0}^{E} j B_j = ES(E) - \sum_{j=0}^{E-1} S(j). \qquad (55)$$

After some algebra, one can show that (53) can be approximated as

$$\sum_{i=0}^{K/L^n-1} J(\boldsymbol{\lambda}|_0^{L-1}(i)) \approx \gamma^2 \frac{|\check{M}|^{\frac{1}{(L-1)n}}}{\mathcal{V}_{(L-1)n}^{\frac{2}{(L-1)n}}} \cdot \frac{(L-1)n}{(L-1)n+2}$$
$$\cdot L^{-n-\frac{2}{L-1}} \cdot K^{1+\frac{2}{(L-1)n}}. \qquad (56)$$

From (34) and (42) we obtain $|\check{M}| = L^n(\frac{K\nu}{\gamma^n})^{2(L-1)}$. It is known that $\mathcal{V}_{(L-1)n}$ can be expressed in terms of $G(S_{Ln-n})$, the normalized second moment of a sphere in $(L-1)n$ dimensions, by

$$\mathcal{V}_{(L-1)n}^{\frac{2}{(L-1)n}} = \frac{1}{G(S_{Ln-n})((L-1)n+2)}. \qquad (57)$$

From (56) and (57) and the expression of $\check{M}$, the distortion d_2 takes the form

$$d_2 \approx (L-1)L^{-\frac{1}{L-1}}(K\nu)^{\frac{2}{n}} G(S_{Ln-n}) K^{\frac{2}{(L-1)n}} \qquad (58)$$

From (51) and (52), it is seen that d_1 and d_2 are similar. Thus, a similar analysis can be performed on d_1, resulting in

$$d_1 \approx L^{-2}(K\nu)^{\frac{2}{n}} G(S_n). \qquad (59)$$

The side distortion $d_{(L,\kappa)}$ is thus fully specified. Note from (46), (58)-(59) that as K increases, d_2 dominates both $d_{(L,L)}$ and d_1. Thus, the side distortion $d_{(L,\kappa)}$ can be further approximated as

$$d_{(L,\kappa)} \approx \frac{L-\kappa}{\kappa} L^{-\frac{L}{L-1}}(K\nu)^{\frac{2}{n}} G(S_{Ln-n}) K^{\frac{2}{(L-1)n}} \qquad (60)$$

as $K \to \infty$.

Finally we present the result of [10] regarding the side distortions. We would like to compare (60) with the expression derived in [10]. Formally, the approximation $\check{d}_{(L,\kappa)}$ of the side distortions is in a form of [10]:

$$\check{d}_{(L,\kappa)} \approx \frac{L-\kappa}{\kappa} L^{-\frac{L}{L-1}}(K\nu)^{\frac{2}{n}} G(S_n)\Phi_{L-1,n} K^{\frac{2}{(L-1)n}}, \quad (61)$$

where

$$\Phi_{L-1,n} = \left(\frac{n+2}{Ln-n+2} \right) \frac{\Gamma(\frac{Ln-n}{2}+1)^{\frac{2}{Ln-n}}}{\Gamma(\frac{n}{2}+1)^{\frac{2}{n}}}. \qquad (62)$$

Note that the only difference between (60) and (61) is the term $G(S_n)\Phi_{L-1,n}$. By using the identity that $G(S_n) = \frac{1}{(n+2)\pi}\Gamma(n/2+1)^{2/n}$, it is immediate that the two expressions (60) and (61) are identical. This result confirms that our geometric analysis is correct.

E. Performance-Loss Evaluation

In this subsection we first study the performance-loss of the index-assignment scheme due to dimensionality. We then characterize the gap between the lower-bound approximation (24) for $\kappa = 1$ and that of the index-assignment scheme. We find that as the quantization dimensionality $n \to \infty$, the gap approaches zero.

We study the relationship between rates and distortions. First, the central distortion can be expressed in terms of R_c as

$$d_{(L,L)} \approx G(\Lambda_c)e^{2(h(f)-R_c)}. \qquad (63)$$

Let $K = e^{nb(L-1)R}$, $b \in (0,1)$. It follows from (45) that $R_c \approx R[1+b(L-1)]$. On substituting the expression for R_c into (63) we arrive at

$$d_{(L,L)} \approx G(\Lambda_c)e^{2h(f)-2R[1+b(L-1)]}. \qquad (64)$$

By utilizing (44) and the expression for K, (60) can be rewritten as

$$d_{(L,\kappa)} \approx \frac{L-\kappa}{\kappa} L^{-\frac{L}{L-1}} G(S_{Ln-n})e^{2h(f)-2R(1-b)}. \qquad (65)$$

The parameter b controls the amount of redundant information between the L descriptions. Interestingly, the side distortions $d_{(L,\kappa)}$, $1 \le \kappa < K$ are characterized by $G(S_{Ln-n})$, the normalized second moment of a sphere in $Ln-n$ dimensions. The product of the distortions over all $1 \le i \le L$ takes the form of

$$\prod_{i=1}^{L} d_{(L,i)} \approx L^{-L} G(\Lambda_c)[G(S_{Ln-n})]^{L-1} e^{2Lh(f)-2RL}. \quad (66)$$

It is seen that the parameter b is not involved in the product, which is consistent with the two-channel results in [6].

Considering the side distortion $d_{(L,\kappa)}$ in (65), when κ increases from 1 to $L-1$, the side distortion is reduced by a factor $\frac{L-\kappa}{\kappa}$. However, the distortion reduction from $L-1$ to L exhibits a singularity. This might be due to the decoding inconsistency in the system.

It is known that a good lattice such that $\lim_{n\to\infty} G(\Lambda) = G(S_\infty)$ exists [20], which simultaneously guarantees that the minimum central and side distortions are achieved. This allows us to study the distortion loss due to dimensionality. From (64), the loss for $d_{(L,L)}$ can be expressed as

$$\lim_{R\to\infty} d_{(L,L)}(R,n)/d_{(L,L)}(R,\infty) = 2\pi e G(\Lambda_c).$$

This confirms that the loss in central distortion is lattice dependent, but channel-number independent. By considering (65), the side distortion loss takes the form of

$$\lim_{R\to\infty} d_{(L,\kappa)}(R,n)/d_{(L,\kappa)}(R,\infty) = 2\pi e G(S_{Ln-n}),$$

where $1 \le \kappa < L$. Thus, on the other hand, the side distortion loss is channel-number dependent, but lattice-independent. This is due to the approximation we introduced for simple characterization of the side distortions. Again, a singularity appears from $\kappa = L - 1$ to L. Fig. 3 displays the distortion loss vs dimensionality for different numbers of channels.
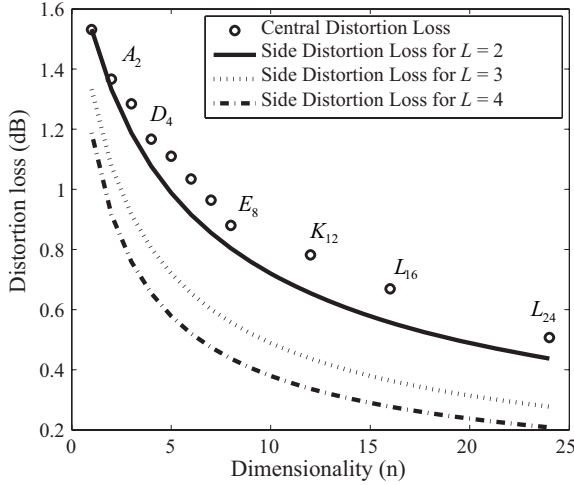

Fig. 3. The central and side distortion loss as a function of the lattice dimensionality n. The loss in central distortion is measured by using the best known lattices for quantization [19].

Finally we assess the performance loss of the MDLVQ scheme w.r.t. the lower-bound approximation. In particular, we specify κ to be 1 in the lower-bound approximation (24). As explained in subsection III-B, the main reason for setting $\kappa = 1$ is that the considered MD scheme exploits the averaging operation (30) for decoding. We consider a memoryless Gaussian source with variance σ_x^2. In this case, $h(f) = \frac{1}{2}\log(2\pi e \sigma_x^2) = \frac{1}{2}\log(\sigma_x^2/G(S_\infty))$. From (64) and (65), the distortion product $d_{(L,1)}^{L-1} d_{(L,L)}$ is given by

$$d_{(L,1)}^{L-1} d_{(L,L)} \approx \left[(L-1)^{L-1} L^{-L} \sigma_x^{2L} e^{-2LR} \frac{G(\Lambda_c)}{G(S_\infty)} \right. \left. \cdot \left(\frac{G(S_{Ln-n})}{G(S_\infty)} \right)^{L-1} \right]. \tag{67}$$

Note that the expression of the side distortion in (65) is derived by assuming a high index value K, implying that

$d_{(L,1)} \gg d_{(L,L)}$. We will therefore be using the lower bound approximation (24) for comparison. One observes that the performance gap between (67) and (24) is only related to $G(\Lambda_c)$ and $G(S_{Ln-n})$. This implies that when $d_{(L,1)} \gg d_{(L,L)}$, the performance of the MDLVQ converges to the theoretical lower bound as $n \to \infty$.

IV. CONCLUSION

We presented a simple lower-bound approximation for L-channel symmetric MD problem with two levels of receivers (one with the central receiver and the other with the receivers receiving a particular number of descriptions) for a scalar Gaussian source. We found that if the central distortion is much smaller than the side distortion, the optimal MD system under high-rate assumption has the property that the product of a function of the side distortion and the central distortion is asymptotically independent of the redundancy between the descriptions. This property can be utilized as a tool to evaluate the efficiency of practical MD systems. We used it to investigate the coding efficiency of an MDLVQ system and observed that the quantization method yields a coder that is asymptotically optimal with the dimensionality and rate.

APPENDIX A
MATRIX LEMMAS

In this appendix, we present some useful matrix lemmas that will be used in the paper.

Lemma A.1 ([21], Theorem 2.5): Let $\mathbf{A}$ be an $m \times m$ nonsingular matrix and $\mathbf{B}$ be an $n \times n$ nonsingular matrix and let $\mathbf{C}$ and $\mathbf{D}$ be $m \times n$ and $n \times m$ matrices, respectively. If the matrix $\mathbf{A} + \mathbf{CBD}$ is nonsingular, then

$$(\mathbf{A}+\mathbf{BCD})^{-1} = \mathbf{A}^{-1} - \mathbf{A}^{-1}\mathbf{C}(\mathbf{B}^{-1}+\mathbf{DA}^{-1}\mathbf{C})^{-1}\mathbf{DA}^{-1}.$$

Lemma A.2 ([8], Lemma 3): Let $\mathbf{K}_w$ be given by (1). Then

$$(1,\ldots,1)\mathbf{K}_w^{-1}(1,\ldots,1)^t = L[\sigma^2 - (L-1)a]^{-1}. \tag{68}$$

Lemma A.3: Let $\mathbf{K}_w$ be given by (1). Then

$$|\mathbf{K}_w| = |\sigma^2 - (L-1)a||\sigma^2 + a|^{L-1}. \tag{69}$$

Proof:

$$|\mathbf{K}_w|$$
$$= |\text{diag}(\sigma^2 + a, \ldots, \sigma^2 + a) - (1,\ldots,1)^t a(1,\ldots,1)|$$
$$= |\mathbf{I}_L - (a,\ldots,a)^t \cdot ((\sigma^2+a)^{-1}, \ldots, (\sigma^2+a)^{-1})|$$
$$\quad \cdot |\sigma^2 + a|^L$$
$$\overset{(a)}{=} |1 - ((\sigma^2+a)^{-1}, \ldots, (\sigma^2+a)^{-1}) \cdot (a,\ldots,a)^t|$$
$$\quad \cdot |\sigma^2 + a|^L$$
$$= |\sigma^2 + a|^{L-1}|\sigma^2 - (L-1)a|.$$

In the above derivations, (a) follows from the determinant identity $|\mathbf{I}_m - \mathbf{A}_{m\times n}\mathbf{B}_{n\times m}| = |\mathbf{I}_n - \mathbf{B}_{n\times m}\mathbf{A}_{m\times n}|$. $\blacksquare$

REFERENCES

[1] A. A. E. Gamal and T. M. Cover, "Achievable Rates for Multiple Descriptions," *IEEE Trans. Inform. Th.*, vol. 28, no. 6, pp. 851–857, 1982.

[2] L. Ozarow, "On a Source-Coding Problem with Two Chnnels and Three Receivers," *Bell system Technical Journal*, vol. 59, no. 10, pp. 1909–1921, 1980.

[3] R. Zamir, "Gaussian Codes and Shannon Bounds for Multiple Descriptions," *IEEE Trans. Inform. Theory*, vol. 45, no. 7, pp. 2629–2636, 1999.

[4] J. Østergaard, J. Jensen, and R. Heusdens, "n-Channel Entropy-Constrained Multiple-Description Lattice Vector Quantization," *IEEE Trans. Inform. Th.*, vol. 52, no. 5, pp. 1956–1973, 2006.

[5] V. A. Vaishampayan and J.-C. Batllo, "Asymptotic Analysis of Multiple Description Quantizers," *IEEE Trans. Inform. Th.*, vol. 44, no. 1, pp. 278–284, 1998.

[6] V. A. Vaishampayan, N. Sloane, and S. Servetto, "Multiple Description Vector Quantization with Lattice Codebooks: Design and Analysis," *IEEE Trans. Inform. Theory*, vol. 47, no. 5, pp. 1718–1734, 2001.

[7] R. Venkataramani, G. Kramer, and V. K. Goyal, "Multiple Description Coding with Many Channels," *IEEE Trans. Inform. Theory*, vol. 49, no. 9, pp. 2106–2114, 2003.

[8] H. Wang and P. Viswanath, "Vector Gaussian Multiple Description With Individual and Central Receivers," *IEEE Trans. Inform. Theory*, vol. 53, no. 6, pp. 2133–2153, 2007.

[9] ——, "Vector Gaussian Multiple Description with Two Levels of Receivers," *IEEE Trans. Inform. Theory*, vol. 55, no. 1, pp. 401–410, 2009.

[10] X. Huang and X. Wu, "Optimal Design of Multiple Description Lattice Vector Quantizers," *submitted to IEEE Trans. Inform. Theory*, 2006.

[11] J. Chen, C. Tian, T. Berger, and S. S. Hemami, "Mutiple Description Quantization via Gram-Schmidt Orthogonalization," *IEEE Trans. Inform. Theory*, vol. 52, no. 12, pp. 5197–5217, 2006.

[12] X. Zhang, J. Chen, S. B. Wicker, and T. Berger, "Successive Coding in Multiuser Information Theory," *IEEE Trans. Inform. Theory*, vol. 53, no. 6, pp. 2246–2254, 2007.

[13] J. Østergaard and R. Zamir, "Multiple Descriptions by Dithered Delta-Sigma Quantization," *IEEE Trans. Inform. Theory*, vol. 55, no. 10, pp. 4661–4675, 2009.

[14] G. Zhang, J. Klejsa, and W. B. Kleijn, "Analysis of K-Channel Multiple Description Quantization," in *Data Compression Conference*, 2009, pp. 53–62.

[15] R. A. Horn and C. R. Johnson, *Matrix Analysis*. Cambridge University Press, 1990.

[16] T. Kailath, A. Sayed, and B. Hassibi, *Linear Estimation*, 1st ed. New Jersey: Prentice Hall, 2000.

[17] V. A. Vaishampayan and J.-C. Batllo, "On Reducing Granular Distortion in Multiple Description Quantization," in *Proc. IEEE Int. Symp. Information Thoery*, 1998.

[18] A. Gersho, "Asymptotically Optimal Block Quantization," *IEEE Trans. Inf. Theory*, vol. 25, no. 4, pp. 373–380, 1979.

[19] J. H. Conway and N. J. A. Sloane, *Sphere Packing, Lattces and Groups*, 3rd ed. Springer, 1998.

[20] U. Erez, S. Litsyn, and R. Zamir, "Latttices Which are Good for (Almost) Everything," *IEEE. Trans. Inf. Theory*, vol. 51, no. 10, pp. 3401–3416, 2005.

[21] F. Zhang, *Matrix Theory: Basic Results and Techniques*. Springer, 1999.

Jan Østergaard (S'98 – M'99) received the M.Sc. degree in electrical engineering from Aalborg University, Aalborg, Denmark, in 1999 and the Ph.D. degree (*cum laude*) in electrical engineering from Delft University of Technology, Delft, The Netherlands, in 2007. From 1999 to 2002, he worked as an R&D engineer at ETI A/S, Aalborg, Denmark, and from 2002 to 2003, he worked as an R&D engineer at ETI Inc., Virginia, United States. Between September 2007 and June 2008, he worked as a post-doctoral researcher in the Centre for Complex Dynamic Systems and Control, School of Electrical Engineering and Computer Science, The University of Newcastle, NSW, Australia. From June 2008 to March 2011, he worked as a post-doctoral researcher at Aalborg University, Aalborg, Denmark. He has also been a visiting researcher at Tel Aviv University, Tel Aviv, Israel, and at Universidad Técnica Federico Santa María, Valparaíso, Chile. He has received a Danish Independent Research Council's Young Researcher's Award and a fellowship from the Danish Research Council for Technology and Production Sciences. Dr. Østergaard is currently an Associate Professor at Aalborg University, Aalborg, Denmark.

Janusz Klejsa (S'05) received the M.Sc. degree in electronics and telecommunications from the Gdansk University of Technology, Poland, in 2005. He joined the Sound and Image Processing Lab at the Royal Institute of Technology (KTH), Stockholm, Sweden, in 2006, where he is currently working towards the Ph.D. degree. His current research interests include quantizer design, multiple description coding and audio coding applications.

Bastiaan Kleijn is Professor of Electronic Engineering at Victoria University of Wellington, New Zealand since 2010. He is also a Professor at the School of Electrical Engineering at KTH (the Royal Institute of Technology) in Stockholm, Sweden, which he joined in 1996 and where he was until recently Head of the Sound and Image Processing Laboratory. He holds a Ph.D. in Electrical Engineering from Delft University of Technology (Netherlands), a Ph.D. in Soil Science and an M.S. in Physics, both from the University of California, Riverside, and an M.S. in Electrical Engineering from Stanford University. He worked on speech processing at AT&T Bell Laboratories from 1984 to 1996. He was a founder of Global IP Solutions, which was acquired by Google in 2010. He is on the Editorial Board of Signal Processing and has been on the Boards of IEEE Transactions of Speech and Audio Processing, IEEE Signal Processing Letters, IEEE Signal Processing Magazine, and the EURASIP Journal of Applied Signal Processing. He has been a member of several IEEE technical committees, and a Technical Chair of EUSIPCO 2010, ICASSP-99, the 1997 and 1999 IEEE Speech Coding Workshops, and a General Chair of the 1999 IEEE Signal Processing for Multimedia Workshop. He is a Fellow of the IEEE.

Guoqiang Zhang (S'06) received his B.S. degree from University of Science and Technology of China (USTC), Hefei, China, in 2003, his M.Phil. degree from the University of Hong Kong, Pokfulam, Hong Kong, in 2006, and his Ph.D. degree in electrical engineering from KTH-Royal Institute of Technology, Stockholm, Sweden, in 2010. His current research interests include multi-terminal information theory, source coding and sensor networks.